Subject Specific Body Model Creation using MR Fingerprinting

Leeor Alon[1,2], Martijn Cloos[1,2], Assaf Tal[3], Daniel K. Sodickson[1,2], and Christopher M. Collins[1,2]

[1]Center for Advanced Imaging Innovation and Research (CAI2R), New York University School of Medicine, New York, NY, United States, [2]Center for Biomedical Imaging, Department of Radiology, New York University School of Medicine, New York, NY, United States, [3]Weizmann Institute, Rehovot, Israel

TARGET AUDIENCE: Those with a need for patient-specific anatomical body models for safety assurance or other purposes.

INTRODUCTION: Routine in-vivo local SAR estimation currently relies heavily on *a priori* simulations, where MR coils are modeled in the presence of a limited number of pre-existing segmented human body models, such as those of the virtual family [1]. The reason that a small number of available segmented human body models exist is due to the labor intensive process required for proper segmentation of tissue anatomies. In this work, we present a method for semi-automatic creation of segmented body models with of MR fingerprinting [2] to rapidly acquire tissue property maps. MR fingerprinting was used to map T1, T2 and proton density in human subjects, and the information was fed into a k-means clustering algorithm for unsupervised classification of tissues. Preliminary results of the method are shown for thigh and head regions of healthy volunteers.

METHODS: A generalized fingerprinting sequence, consisting of 4 segments, each containing 120 excitations 4.8ms after one another was used [3]. The first and third segments contain RF spoiled gradient echoes that predominantly encode B1 and T1, whereas the other segments also add a T2 relaxation component (no RF spoiling). Collectively, these 480 snapshots capture a distinct signal evolution (fingerprint) that simultaneously identifies the RF-field distributions and tissue properties. To increase T1 accuracy and help decouple transmit phase interactions a strategically chosen delay was inserted between each segment. Interleaving 6 delays, each one can be used to image a different slice for maximum efficiency. A radial sampling strategy was selected using golden angle used to promote incoherence.

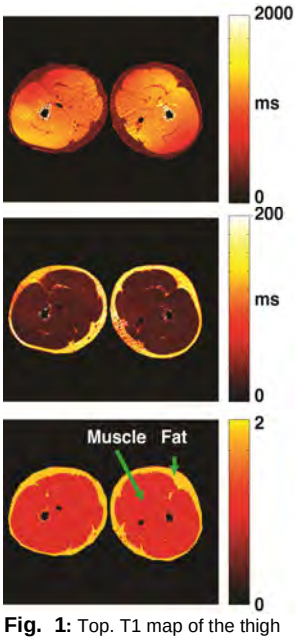

Fig. 1: Top. T1 map of the thigh reconstructed using MR fingerprinting. Middle. T2 map. Bottom. Muscle-fat separation.

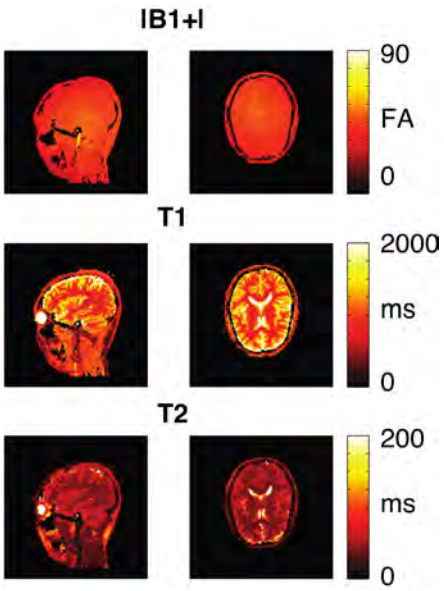

Fig. 2: Sagittal and axial reconstructed |B1+|, T1 and T2 maps of the head.

The spin dynamics of the sequence mentioned above were simulated using a Bloch simulator in MatLab (The MathWorks, Inc., Natick, Massachusetts, United States) in order to create a spin-dynamics dictionary. One hundred spins per RF pulse and gradient waveform were tracked in order to properly capture the spin dynamics. A total of 600,000 combinations of T1's, T2's and B1+'s were used to create the dictionary and computation time was <24 hours in MatLab.

Images of the thigh were acquired with a standard 12-channel body matrix coil in a clinical single-transmit 3 Tesla system (Siemens, Erlangen, Germany). Sequence parameters were: 288x288 matrix, 2.7x2.7mm^2 in-plane resolution and 1.5mm slice. Acquisition time for 6 sagittal slices covering both legs was 1:59 minutes. Images of the whole head were acquired with a standard 20 channel head-neck receive coil in a clinical 3 Tesla system (Siemens, Erlangen, Germany). Sequence parameters were: 128x128 matrix, 2.5x2.5mm^2 in-plane resolution and 5mm slice. Acquisition time for the entire head with 36 slices was 12:45 minutes.

K-space data were reconstructed using a non-uniform Fourier transform (NUFFT) and image fingerprints were matched to the previously calculated spin dynamics dictionary. The best correlation between the fingerprints in the images and the dictionary were used to map T1, T2, B1 and MB1- (magnetization density times the receive sensitivity profile) values of the tissues. After the various tissue contrast maps were computed, the T1 and T2 values of the maps were normalized and fed into a k-means clustering algorithm [4], which is commonly used to solve unsupervised learning classification problems. The number of clusters was defined based on a-priori knowledge of the anatomy scanned. Two and eight clusters were used for segmentation of the thigh and head regions, respectively, and took under one minute.

RESULTS: Figure 1 shows single reconstructed maps of T1 (top) and T2 (middle), as well as the k-means segmentation of muscle and fat (bottom) for an axial slice through the thigh. Figure 2 shows maps of |B1+|, T1, and T2 reconstructed in axial and sagittal planes through the brain. T1 and T2 maps were used as input for the k-means segmentation. Segmentation results are shown in Fig. 3 for axial and sagittal slices of interest where 9 tissues were classified (air/bone, white matter, subcutaneous/orbital fat, muscle, cerebrospinal fluid, aqueous humor, connective tissue, and two layers of gray matter).

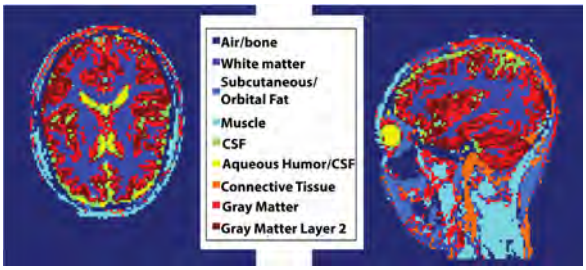

Figure 3: k-means 9 tissue segmentation based on the MR fingerprinting reconstructed T1 and T2 maps.

DISCISSION & CONCLUSION: A semi-automatic method for creation of subject-specific body models with numerous tissues is presented in this work. Conventional methods for segmentation used up until now were labor intensive and involved significant manual intervention. By comparison, this method is significantly faster. Several computational tools have been used in the past for segmentation of the brain region based on using T1 weighted inversion recovery sequences [5] and Fat-water separation techniques [6], however, the classification problems were susceptible to variations in transmit and receive field contrasts and classified only a few tissue types. Because MR fingerprinting was shown to robustly map the T1, T2, MB1- and B1+, we are able to remove B1+ and MB1- nuisance variables from the classification problem, since they are confounding factors and hold very little tissue-specific information (at least for the operating frequency of 3T MR). Because they have similar electrical properties, the inability to distinguish air from bone is not seen as problematic for RF safety assurance. The images presented are still preliminary and further optimization is sought to improve this methodology, specifically improving speed of acquisition with the goal of close-to-real-time image segmentation. Furthermore, as in the brain images presented, partial-averaging affects can create problems for the classification algorithm, thus acquisitions with finer resolution are a work in progress.

REFERENCES: [1] Christ A., et al, Phys Med Biol, 55 (2010), pp. N23-38. [2] Ma, et al., Nature 2013, DOI: 10.1038/nature11971. [3] Cloos et al., ISMRM 2014 #542. [4] Seber, G. A. F. Multivariate Observations. 1984. [5] Friston K et al. Human brain function, 2nd edn. pp 695–706. (2003). [6] Homann H et al., MRM 2011;66:1767-76.